

Out-of-plane dispersion and homogenization in photonic crystal slabs

Zhongping Jian and Daniel M. Mittleman^{a)}

Department of Electrical and Computer Engineering, Rice University, MS-366, P.O. Box 1892, Houston, Texas 77005-1892

(Received 24 May 2005; accepted 19 September 2005; published online 4 November 2005)

We report a measurement of out-of-plane dispersion in two-dimensional photonic crystal slabs. Using terahertz time-domain spectroscopy, we obtain the complex transmission coefficient over a broad spectrum, ranging from the long wavelength (homogeneous) limit up to beyond the first few guided resonances. Despite the absence of a band gap, the out-of-plane dispersion is significant and in addition exhibits a complicated spectral dependence. Calculations of the effective refractive index which assume translational invariance in the direction perpendicular to the slab are in only approximate agreement with the measured homogeneous effective index and dispersion. In contrast, numerical simulations which accurately account for the finite slab thickness give much more accurate predictions. © 2005 American Institute of Physics. [DOI: 10.1063/1.2131195]

The propagation of electromagnetic waves in periodic dielectric structures has become an important area of research. In particular, photonic crystal slabs, with periodicity in two dimensions and finite thickness in the third dimension, are of special interest.¹ In the plane of the periodicity, such structures can exhibit a complete photonic band gap, which can be exploited for a variety of applications.² Recently the propagation of light along the direction *perpendicular* to the plane of periodicity has also attracted much attention. Consideration of out-of-plane propagation is relevant in the coupling between guided and lossy or defect modes.^{3–7} In addition, guided resonances, which couple to freely propagating out-of-plane modes, have recently been the subject of intense study.^{8,9} Such resonances may be used as the basis for novel mirrors or filters^{10–12} or as sensitive displacement sensors.¹³ Despite the significance of the out-of-plane propagation, only a few studies have reported experimental measurements of transmission or reflection spectra,^{3,4,7,12,14,15} and we are aware of no reports of spectral phase measurements. Theories based on plane wave expansion methods have been used to predict the effective refractive index perpendicular to the plane,^{16,17} but experimental confirmation of these predictions is lacking.

Here, we describe measurements of the complex transmission coefficient perpendicular to a photonic crystal slab. Our data span the spectral range from the homogeneous (long wavelength) limit to beyond the first few guided resonances. We find that predictions of the phase of the transmitted radiation, computed using plane wave expansion methods,^{16,17} provide only a qualitative description of the homogeneous limit and the low-frequency dispersion. In contrast, numerical simulations which accurately account for the finite thickness of the slab¹⁸ give better agreement with the measurements. These experimental results emphasize the difficulties in using plane wave methods to describe propagation perpendicular to the slab.

For broadband characterization of photonic crystals, we employ terahertz (THz) time-domain spectroscopy to determine both the transmission amplitude and phase over a wide spectral range.^{19–24} Because of the low frequency of the ra-

diation (100–1000 GHz), photonic crystals can be fabricated which are nearly perfect on the scale of the wavelength, with essentially zero positional or size disorder and negligible interface roughness. We have used deep reactive ion etching to form an array of circular air holes, penetrating all the way through a 305- μm -thick high-resistivity ($>10\text{ k}\Omega\text{ cm}$) silicon wafer.^{23–25} This material exhibits extremely low absorption and a frequency-independent refractive index of $n_{\text{Si}} = 3.418$ throughout the THz range.²⁶ The holes, with diameters of 360 μm , are arranged on a hexagonal lattice with spacing $a = 400\text{ }\mu\text{m}$. The in-plane band structure of this sample, computed using a plane wave expansion method,¹⁶ may be found in Ref. 24. To obtain the transmission coefficient for propagation perpendicular to the plane of the slab, we compare the transmitted THz pulse with the sample in the collimated THz beam to that measured with no sample in the beam path.

A typical set of results is shown in Fig. 1. Figure 1(a) shows the transmission amplitude, which exhibits Fabry-Pérot oscillations at low frequency and shows evidence of three guided resonances at higher frequency.⁸ The solid curve is the result of a simulation using the finite element method (FEM), which reproduces all of these features. Figure 1(b) shows the transmitted phase measured relative to that of no sample in the beam path, $\Delta\phi = \phi_{\text{slab}} - \phi_{\text{air}}$. The phase exhibits a marked nonlinearity, and also shows abrupt jumps due to the guided resonances. Here, the solid curve is the result of a finite-difference time-domain (FDTD) simulation.

As a comparison, we also show the transmission amplitude and relative phase for in-plane propagation, along the ΓM direction (two insets in Fig. 1). Because the thickness of the slab is less than the longest free-space wavelength of our THz pulse, we perform these measurements in a waveguide geometry, with the photonic crystal slab placed inside a parallel plate copper waveguide. Since the lowest-order E -polarized (TM) mode of this waveguide exhibits no cutoff wavelength, all of the measured dispersion can be attributed to the effects of the photonic crystal.²⁷ This geometry has proven to be a powerful tool for broadband waveguide THz spectroscopy.^{23,24,28} We observe that $\Delta\phi$ is nearly linear up to a frequency close to that of the lower edge of the first (partial) photonic band gap, a result which is consistent with

^{a)}Electronic mail: daniel@rice.edu

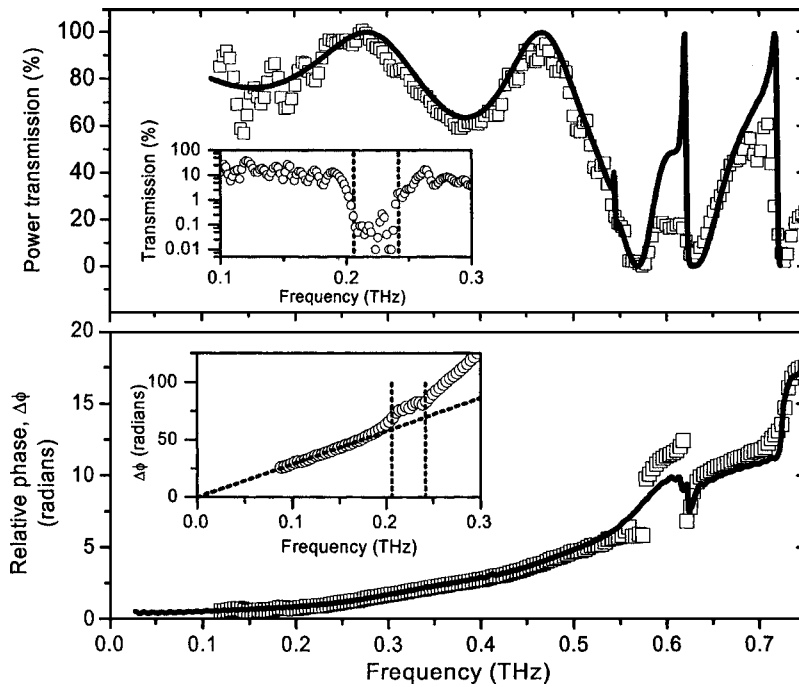


FIG. 1. (a) Power transmission coefficient and (b) relative phase $\Delta\phi$ for transmission perpendicular to the photonic crystal slab. The phase is measured relative to the case of no sample in the THz beam path. In (a), the solid line is the result of a FEM simulation, while in (b), the solid line is a FDTD simulation. Both simulations account for the finite thickness of the sample along the propagation direction, and both reproduce the frequency-dependent features of the data. The two insets show the transmission and relative phase for *in-plane* propagation (TM polarization), along the ΓM direction. The vertical dashed lines indicate the edges of the first (partial) photonic band gap. The slanted dashed line in (b) is a guide to the eye to indicate the linearity (and the zero intercept) of the in-plane phase at low frequencies.

previous in-plane dispersion measurements on similar samples.²⁹⁻³¹

The out-of-plane data of Fig. 1 were obtained with the input polarization oriented along the ΓM axis of the hexagonal lattice. However, as expected,¹⁷ we observe no polarization dependence. Crystals with threefold rotational symmetry (such as ours) are uniaxial in the homogeneous limit, possessing only two distinct effective dielectric constants, one for in-plane and one for out-of-plane propagation.

We can obtain these two frequency-dependent effective parameters from the data of Fig. 1(b) (and inset). However, the oscillatory structure at low frequencies in Fig. 1(a) highlights the need for care in processing the out-of-plane data. These Fabry-Pérot fringes cannot be removed by a simple windowing procedure in the time domain, because the sample is too thin. Instead, we obtain the effective refractive index using a numerical error minimization procedure described previously.³² In our case, because the attenuation (due to guided resonances) is relatively small below ~ 0.5 THz, this procedure leads to only a small modification, but still effectively eliminates Fabry-Pérot effects from the extracted index. We note that this procedure is not required to obtain $n_{\text{eff}}(\omega)$ for in-plane propagation, since in that case the sample is thick enough (20 periods) that the Fabry-Pérot effects can be removed by time-domain filtering.

Figure 2 shows the effective refractive index for out-of-plane propagation, obtained from $\Delta\phi(\omega)$; the inset shows the result for in-plane propagation. We find that the effective in-plane index is equal to the square root of the volume-weighted average dielectric constant, precisely the result predicted by homogenization theory.¹⁷ Deviations from this value occur only for $\omega a/2\pi c > 0.23$, as the frequency approaches the lower edge of the band gap. Despite the absence of a band gap for propagation perpendicular to the slab, the effective out-of-plane index nevertheless also exhibits large dispersion in the frequency range below the first guided resonance. Moreover, the frequency dependence is not simply a smooth increase (as in the case of the in-plane effective index). Finally, the measured low-frequency limiting value,

$n_{\text{meas}} = 1.73 \pm 0.07$, is notably larger than the calculated homogeneous limit of $n_{\text{hom}} = 1.6448$.

In Fig. 2, we also show computations of both the homogeneous limit (dashed line) and the dispersion (dotted curve), obtained using analytic theories based on plane wave expansion of the spatially varying dielectric.^{1,16,17,33} Such theories rely on the assumption of translational invariance along the direction perpendicular to the slab; in other words, the finite thickness of the slab is not considered. As a result, the agreement with experiment is only qualitative.¹⁸ In contrast, a FDTD simulation (solid curve), which includes a realistic representation of the sample, accurately reproduces both the

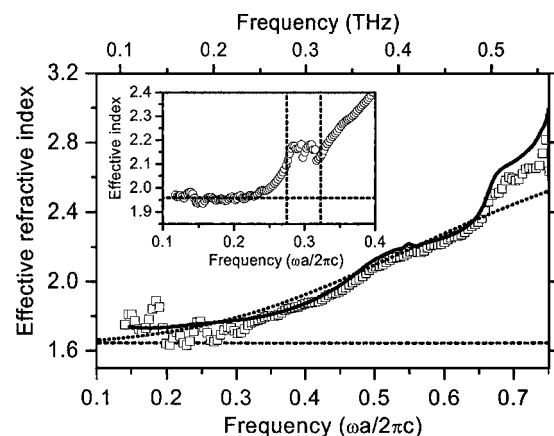


FIG. 2. Effective refractive index vs frequency, for propagation normal to the plane of the photonic crystal slab, for the frequency range below the first guided resonance. The horizontal dashed line indicates the predicted homogeneous limit of $n_{\text{hom}} = 1.6448$, which is smaller than the measured low-frequency value of $n_{\text{meas}} = 1.73 \pm 0.07$. The dotted curve shows the dispersion predicted by a band structure calculation for out-of-plane propagation, based on a plane wave method (see Ref. 16). The solid curve is the FDTD simulation from Fig. 1. In the inset, the equivalent result is displayed for propagation in the plane of the slab. In contrast to the out-of-plane result, the predicted homogeneous value of $n_{\text{hom}} = 1.9585$ (horizontal dashed line) is precisely consistent with the measurement at low frequencies, $n_{\text{meas}} = 1.958 \pm 0.011$. Deviations are observed only as the frequency approaches that of the band gap (vertical dashed lines).

frequency-dependent dispersion and the low-frequency limit of the out-of-plane effective index.

In conclusion, we have described an experimental measurement of the out-of-plane dispersion and homogenization of photonic crystal slabs and found notable discrepancies with existing theoretical treatments. Because numerical simulations (which account for the finite thickness of the slab) give better agreement with measurements, the discrepancies would seem to be a consequence of the lack of translational symmetry along the propagation direction, which is not considered in many theoretical treatments. This highlights the unique challenge of describing propagation perpendicular to the slab, even in the long wavelength limit. This configuration is not particularly amenable to homogenization, because the wave does not sample a large number of unit cells.¹⁷ For the case of a slab of finite thickness, this difficulty is not limited strictly to normal incidence propagation—indeed, for all incident angles $\theta < \theta_0$, the propagating wave samples less than one unit cell before exiting the medium. Here, θ_0 is a critical angle determined by the effective index and the ratio of the slab thickness to the lattice period. For the sample described here ($n_{\text{hom}} \sim 1.73, d/a = 0.763$), we find $\sin \theta_0 > 1$, which implies that *no* out-of-plane incident wave, arriving from *any* external angle, samples the homogeneous infinite-slab limit. For slabs of finite thickness, a more sophisticated theoretical treatment is required to accurately describe the out-of-plane dispersion and homogenization.

This work has been supported in part by the National Science Foundation.

¹S. G. Johnson, S. Fan, P. R. Villeneuve, J. D. Joannopoulos, and L. A. Kolodziejski, *Phys. Rev. B* **60**, 5751 (1999).

²J. D. Joannopoulos, R. D. Meade, and J. N. Winn, *Photonic Crystals: Molding the Flow of Light* (Princeton University Press, Princeton, NJ, 1995).

³M. Kanskar, P. Paddon, V. Pacradouni, R. Morin, A. Busch, J. F. Young, S. R. Johnson, J. MacKenzie, and T. Tiedje, *Appl. Phys. Lett.* **70**, 1438 (1997).

⁴V. N. Astratov, I. S. Culshaw, R. M. Stevenson, D. M. Whittaker, M. S. Skolnick, T. F. Krauss, and R. M. D. L. Rue, *J. Lightwave Technol.* **17**, 2050 (1999).

⁵A. A. Erchak, D. J. Ripin, S. Fan, P. Rakich, J. D. Joannopoulos, E. P. Ippen, G. S. Petrich, and L. A. Kolodziejski, *Appl. Phys. Lett.* **78**, 563 (2001).

⁶W. Bogaerts, P. Bienstman, D. Taillaert, R. Baets, and D. De Zutter, *IEEE Photonics Technol. Lett.* **13**, 565 (2001).

⁷S. Foteinopoulou, A. Rosenberg, M. M. Sigalas, and C. M. Soukoulis, *J. Appl. Phys.* **89**, 824 (2001).

⁸S. Fan and J. D. Joannopoulos, *Phys. Rev. B* **65**, 235112 (2002).

⁹S. Fan, W. Suh, and J. D. Joannopoulos, *J. Opt. Soc. Am. A* **20**, 569 (2003).

¹⁰W. Suh and S. Fan, *Opt. Lett.* **28**, 1763 (2003).

¹¹W. Suh and S. Fan, *Appl. Phys. Lett.* **84**, 4905 (2004).

¹²V. Lousse, W. Suh, O. Kilic, S. Kim, O. Solgaard, and S. Fan, *Opt. Express* **12**, 1575 (2004).

¹³W. Suh, M. F. Yanik, O. Solgaard, and S. Fan, *Appl. Phys. Lett.* **82**, 1999 (2003).

¹⁴M. C. Netti, A. Harris, J. J. Baumberg, D. M. Whittaker, M. B. D. Charlton, M. E. Zoorob, and G. J. Parker, *Phys. Rev. Lett.* **86**, 1526 (2001).

¹⁵O. Kilic, S. Kim, W. Suh, Y.-A. Peter, A. S. Sudbø, M. F. Yanik, S. Fan, and O. Solgaard, *Opt. Lett.* **29**, 2782 (2004).

¹⁶S. G. Johnson and J. D. Joannopoulos, MIT Photonic Bands package, <http://ab-initio.mit.edu/mpb> (1999).

¹⁷A. A. Krokhin, P. Halevi, and J. Arriaga, *Phys. Rev. B* **65**, 115208 (2002).

¹⁸A. Di Falco, C. Conti, and G. Assanto, *J. Lightwave Technol.* **22**, 1748 (2004).

¹⁹E. Ozbay, E. Michel, G. Tuttle, R. Biswas, K. M. Ho, J. Bostak, and D. M. Bloom, *Opt. Lett.* **19**, 1155 (1994).

²⁰A. Chelnokov, S. Rowson, J.-M. Lourtioz, L. Duvaillaret, and J.-L. Coutaz, *Electron. Lett.* **33**, 1981 (1997).

²¹H. Kitahara, N. Tsumura, H. Kondo, M. W. Takeda, J. W. Haus, Z. Yuan, N. Kawai, K. Sakoda, and K. Inoue, *Phys. Rev. B* **64**, 045202 (2001).

²²H. Han, H. Park, M. Cho, and J. Kim, *Appl. Phys. Lett.* **80**, 2634 (2002).

²³Z. Jian, J. Pearce, and D. M. Mittleman, *Opt. Lett.* **29**, 2067 (2004).

²⁴Z. Jian, J. Pearce, and D. M. Mittleman, *Semicond. Sci. Technol.* **20**, 300 (2005).

²⁵N. Jukam and M. S. Sherwin, *Appl. Phys. Lett.* **83**, 21 (2003).

²⁶D. Grischkowsky, S. Keiding, M. van Exter, and C. Fattinger, *J. Opt. Soc. Am. B* **7**, 2006 (1990).

²⁷R. Mendis and D. Grischkowsky, *Opt. Lett.* **26**, 846 (2001).

²⁸J. Zhang and D. Grischkowsky, *Opt. Lett.* **29**, 1617 (2004).

²⁹W. Park and C. J. Summers, *Opt. Lett.* **27**, 1397 (2002).

³⁰M. C. Netti, C. E. Finlayson, J. J. Baumberg, M. D. B. Charlton, M. E. Zoorob, J. S. Wilkinson, and G. J. Parker, *Appl. Phys. Lett.* **81**, 3927 (2002).

³¹K. Inoue, N. Kawai, Y. Sugimoto, N. Carlsson, N. Ikeda, and K. Asakawa, *Phys. Rev. B* **65**, 121308 (2002).

³²L. Duvaillaret, F. Garet, and J.-L. Coutaz, *IEEE J. Sel. Top. Quantum Electron.* **2**, 739 (1996).

³³P. Halevi, A. A. Krokhin, and J. Arriaga, *Phys. Rev. Lett.* **82**, 719 (1999).